



*Citation for published version:*

Slavcheva, G 1990, 'Slow ramp - voltage technique for investigation of breakdown voltage distribution in thin plasma nitrided SiO<sub>2</sub> films', *Thin Solid Films*, vol. 192, no. 1, pp. 41-57 . [https://doi.org/10.1016/0040-6090\(90\)90477-U](https://doi.org/10.1016/0040-6090(90)90477-U)<sup>2</sup>

*DOI:*

[10.1016/0040-6090\(90\)90477-U](https://doi.org/10.1016/0040-6090(90)90477-U)

*Publication date:*

1990

*Document Version*

Early version, also known as pre-print

[Link to publication](#)

## University of Bath

### Alternative formats

If you require this document in an alternative format, please contact:  
[openaccess@bath.ac.uk](mailto:openaccess@bath.ac.uk)

#### General rights

Copyright and moral rights for the publications made accessible in the public portal are retained by the authors and/or other copyright owners and it is a condition of accessing publications that users recognise and abide by the legal requirements associated with these rights.

#### Take down policy

If you believe that this document breaches copyright please contact us providing details, and we will remove access to the work immediately and investigate your claim.

## SLOW RAMP VOLTAGE TECHNIQUE FOR INVESTIGATION OF BREAKDOWN VOLTAGE DISTRIBUTION IN THIN PLASMA-NITRIDED SiO<sub>2</sub> FILMS

G. SLAVCHEVA

*Institute of Solid State Physics, Bulgarian Academy of Sciences, Blvd. Lenin 72, 1784 Sofia (Bulgaria)*

(Received October 9, 1989; revised April 24, 1990; accepted May 14, 1990)

The slow ramp current–voltage characteristics of NH<sub>3</sub>–plasma-nitrided samples of thermally grown chlorine SiO<sub>2</sub>,  $d = 200\text{--}350 \text{ \AA}$ , have been measured and the breakdown voltage statistics determined. The characteristics of the breakdown voltage distribution of a double layer and completely nitrided samples have been derived. Evidence is given that the dominant conductivity mechanism is contact-limited Fowler–Nordheim emission.

---

### 1. INTRODUCTION

Although currently used SiO<sub>2</sub> and Si<sub>3</sub>N<sub>4</sub> films have been subject to thorough investigation and have proved their features appropriate for gate and tunnelling insulators and passivation films, recently more interest has been paid to silicon oxynitride films<sup>1,2</sup>. The latter are a consequence of the possibility of gradually changing their composition from SiO<sub>2</sub> to Si<sub>3</sub>N<sub>4</sub> by varying the processing conditions and thus obtaining different electrical and optical properties. On scaling down the dimensions of metal–oxide–silicon (MOS) devices, the gate and tunnelling oxide thicknesses are reduced and the thin SiO<sub>2</sub> films are not able to meet the requirements of very-large-scale integrated (VLSI) circuits because of their decreased dielectric strength and instabilities. The replacement of gate SiO<sub>2</sub> by Si<sub>3</sub>N<sub>4</sub> is reasonable because the nitride films serve as a barrier to impurity diffusion and contamination into the underlying silicon substrate and are chemically more inert than SiO<sub>2</sub><sup>3,4</sup>. On the other hand, a disadvantage of Si<sub>3</sub>N<sub>4</sub> films is the generation of structure defects and traps in the forbidden gap during the fabrication process. A compromise to this is offered by oxynitride films, whose properties reported recently are even superior to those of SiO<sub>2</sub> (see *e.g.* ref. 2). These properties are strongly correlated to the processing conditions, which is the reason for searching for the optimum technology regime.

The purpose of this paper is to investigate the dielectric breakdown voltage and its correlation with the conditions of plasma-enhanced nitridation of thin (200–350 Å) SiO<sub>2</sub> films.

## 2. EXPERIMENT

The samples examined have been fabricated on p-Si (100) wafers with  $\rho = 13\text{--}17\ \Omega\text{cm}$ . They have been thermally oxidized in dry  $\text{O}_2 + 4\% \text{HCl}$  at  $T = 900\text{--}1000^\circ\text{C}$  without any additional high temperature  $\text{N}_2$  annealing. Oxide layers 220 and 340 Å thick have been grown. The oxidized samples have been treated with  $\text{NH}_3$  plasma under different processing temperature and time regimes.  $\text{NH}_3$  plasma exposure has been carried out in an r.f. (13.56 MHz) planar plasma reactor (Reinberg type). The ammonia used was ultrahigh purity grade (Matheson Gas products). The samples have been placed on a grounded electrode whose temperature  $T_s$  has been changed in the range 293–573 K. The r.f. power density was  $0.1\ \text{W cm}^{-2}$  at a gas pressure of 133 Pa. Plasma treatment was performed for durations  $t_e$  between 2 and 100 min. The oxide and oxynitride thicknesses have been measured by an ellipsometer. No change in thickness has been detected after plasma nitridation for all plasma regimes used. This is in agreement with the data obtained in ref. 5 for pyrolytically nitrided  $\text{SiO}_2$ .

Metal-insulator-silicon (MIS) capacitors with oxynitride film have been prepared with a vacuum-evaporated aluminium gate electrode. The electrode area of the capacitors was  $1.96 \times 10^{-3}\ \text{cm}^2$ . Current-voltage measurements have been taken at room temperature in the dark with a negatively biased gate, corresponding to accumulation of the p-Si substrate.

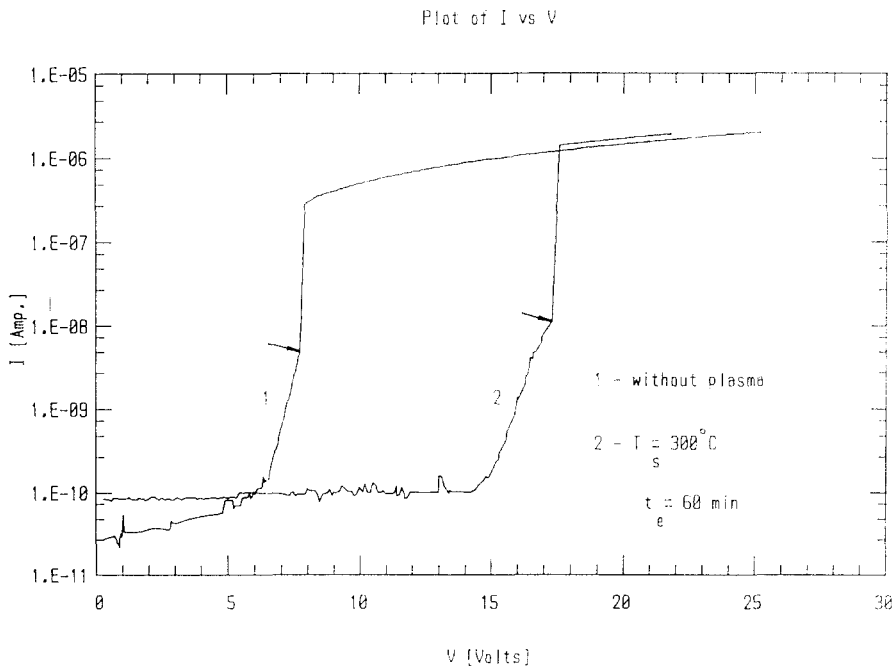


Fig. 1.  $I$ - $V$  characteristics of (1) as-grown  $\text{SiO}_2$  sample with oxide thickness  $d = 340\ \text{\AA}$  and (2)  $\text{NH}_3$ -plasma-treated sample at  $T_s = 300^\circ\text{C}$  and  $t_e = 60\ \text{min}$ . The breakdown voltage points are indicated by arrows.

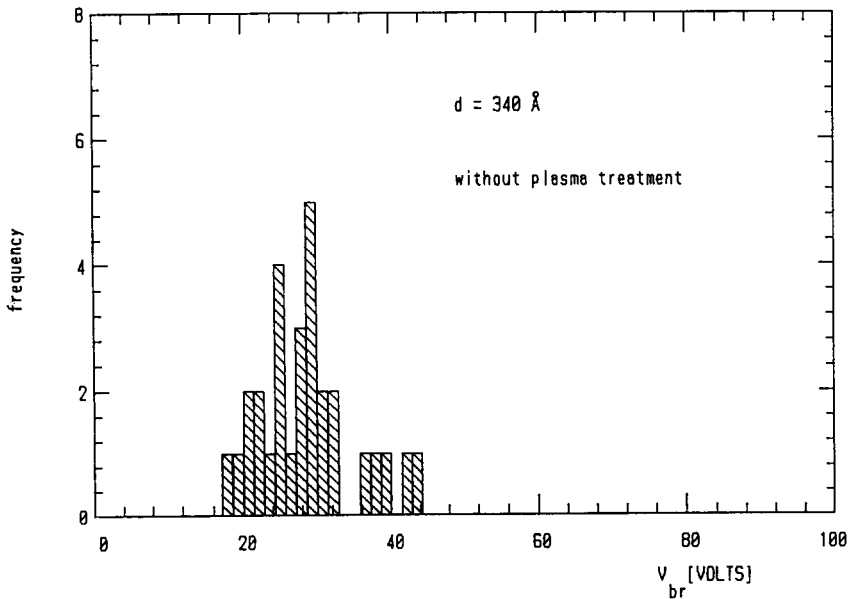
Breakdown voltages have been measured by the slow ramp voltage technique in order to meet the requirement of quasi-stationarity. The ramp rate has been kept constant for every sample and varied between 0.1 and 0.25 V s<sup>-1</sup>. The data have been measured via a Programmable Keithley connected to a microcomputer. Typical I-V characteristics are presented in Fig. 1 to illustrate the pre-breakdown and breakdown behaviour.

The initial current below 1 × 10<sup>-10</sup> A is the displacement current through the capacitor structure,  $I = C_{ox} dV/dt = \alpha C_{ox}$ , where  $\alpha$  is the ramp rate (V s<sup>-1</sup>). The points where irreversible destructive breakdown occurs are shown by arrows in Fig. 1. The breakdown condition has been chosen as the value of voltage at which the current grows abruptly to the value corresponding to the current across the resistor R<sub>b</sub> in series with the examined structure (R<sub>b</sub> = 10 MΩ) and the I-V characteristic starts to obey Ohm's law on a semilogarithmic scale. That means that the structure resistance becomes zero (i.e. it is short circuited).

As shown in Fig. 1, the conductance behaviour of the reference sample and of the plasma-nitrided sample is similar. The conductance mechanism will be discussed in the next section.

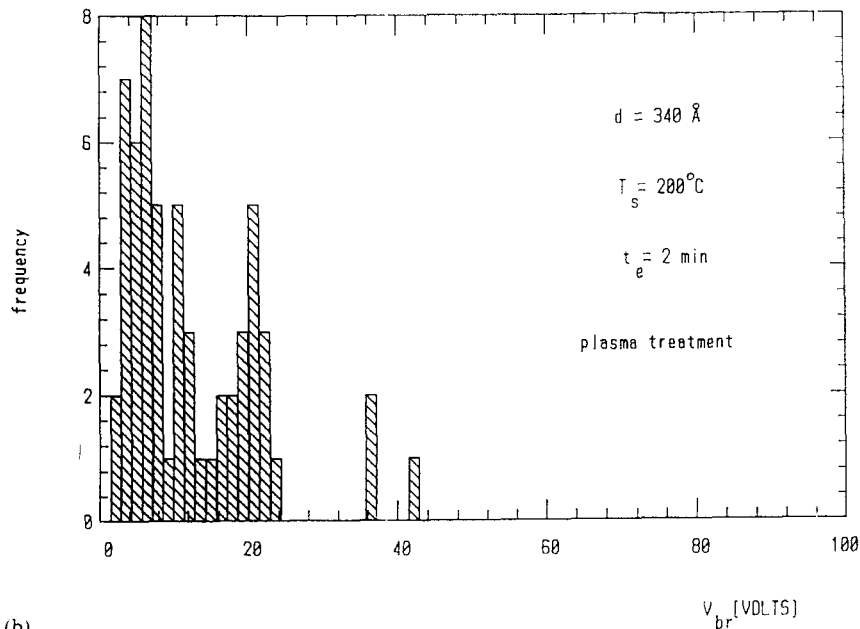
3. DATA PROCESSING AND DISCUSSION OF THE RESULTS

In order to determine the breakdown point accurately, a computer programme has been developed which obtains breakdown voltage and current values directly from an I-V curve and stores them in files. These data are used to plot histograms of the breakdown voltages. From these histograms the important parameters of the breakdown voltage distribution have been obtained: the mean breakdown voltage

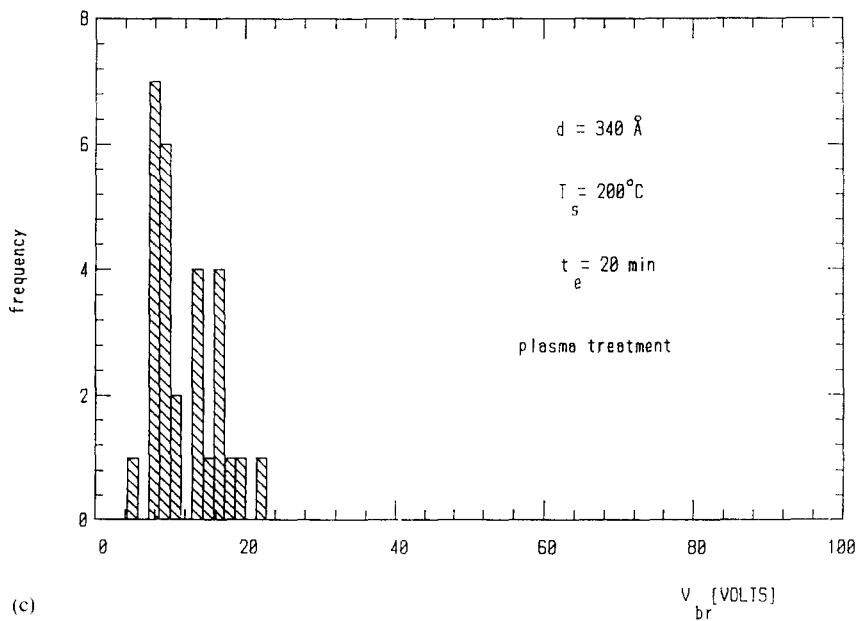


(a)

Fig. 2 (continued).



(b)



(c)

Fig. 2. Histograms of (a) as-grown  $\text{SiO}_2$  sample with oxide thickness  $d = 340 \text{ \AA}$  and (b), (c) two samples processed at the same substrate temperature  $T_s = 200^\circ\text{C}$  but for different durations of plasma exposure. (a)  $t_e = 2 \text{ min}$ , (b)  $t_e = 20 \text{ min}$ .

TABLE I  
CHARACTERISTIC PARAMETERS OF THE BREAKDOWN VOLTAGE DISTRIBUTION FOR ALL SAMPLES  
INVESTIGATED

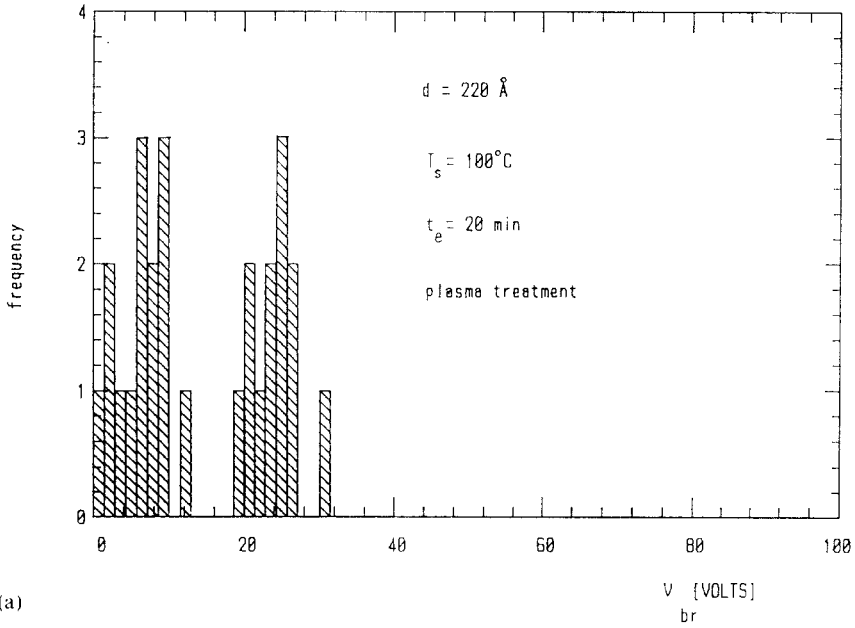
Technology conditions	$d$ (Å)	$\bar{V}_{br}$ (V)	$\sigma$	$max V_{br}$	median	$E_{br}$ (V cm <sup>-1</sup> )	$Q_{bd}$ (cm <sup>-2</sup> )
As-grown SiO <sub>2</sub> ( $d = 340$ Å)	340	28.586	6.43	29.286	28.252	$8.41 \times 10^6$	$5.10 \times 10^{16}$
NH <sub>3</sub> plasma $T_s = 200$ °C $t_e = 2$ min	340	12.263	8.84	6.429	9.873	$3.60 \times 10^6$	$1.67 \times 10^{16}$
NH <sub>3</sub> plasma $T_s = 200$ °C $t_e = 20$ min	340	11.914	4.15	7.857	10.108	$3.50 \times 10^6$	$3.37 \times 10^{15}$
NH <sub>3</sub> plasma $T_s = 300$ °C $t_e = 20$ min	220	3.479	3.96	2.143	2.069	$1.58 \times 10^6$	$5.87 \times 10^{12}$
NH <sub>3</sub> plasma $T_s = 300$ °C $t_e = 30$ min	220	2.421	2.44	2.143	2.045	$1.1 \times 10^6$	$6.73 \times 10^{14}$
NH <sub>3</sub> plasma $T_s = 100$ °C $t_e = 20$ min	220	14.391	9.41	9.3	10.950	$6.54 \times 10^6$	$1.42 \times 10^{13}$
NH <sub>3</sub> plasma $T_s = 300$ °C $t_e = 100$ min	220	10.216	11.52	2.143	4.591	$0.97 \times 10^6$	$6.79 \times 10^{14}$
NH <sub>3</sub> plasma $T_s = 300$ °C $t_e = 60$ min	340	9.462	5.41	15.00	9.350	$2.78 \times 10^6$	$3.73 \times 10^{13}$

$\bar{V}_{br}$  (or breakdown field  $E_{br}$ ); the maximum breakdown voltage  $max V_{br}$ ;  $\sigma$ , the standard deviation of the distribution; the median of the distribution; and  $Q_{bd}$ , the total charge accumulated in the capacitor until breakdown.

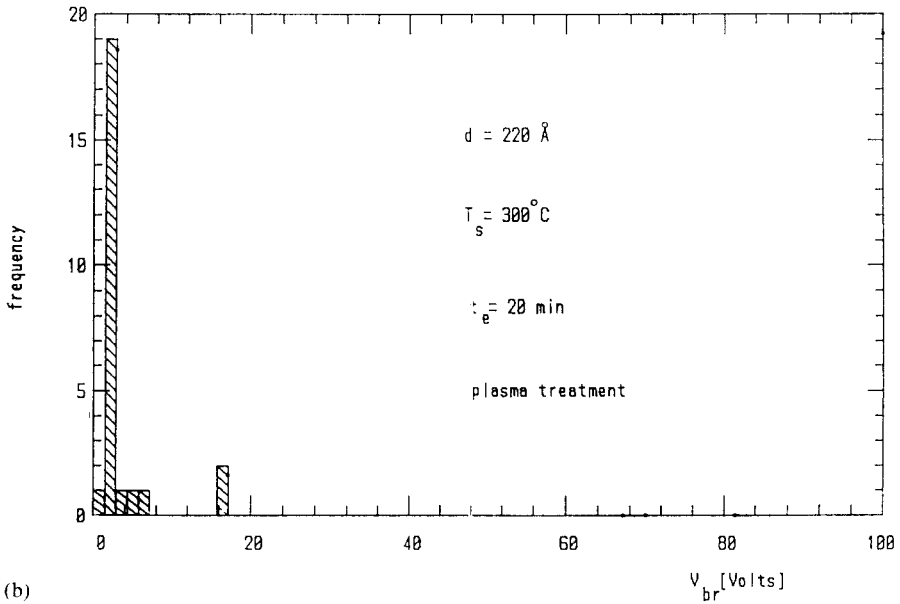
Figure 2 shows three histograms from which the dependence on  $t_e$  at a constant substrate temperature of 200 °C could be tracked (characteristic parameters of the films for all cases investigated are presented in Table I). The mean breakdown fields for the as-grown reference SiO<sub>2</sub> samples of thicknesses  $d = 220$  and 340 Å are approximately equal at about  $1 \times 10^7$  V cm<sup>-1</sup>, which is a typical value for high quality SiO<sub>2</sub> films.

After plasma treatment the films shown in Fig. 2 have an index of refraction  $n = 1.46$ – $1.47$ . These values are very close to those of SiO<sub>2</sub> and correspond to compositions practically the same as for the untreated oxide. As can be seen (Fig. 2, Table I), the mean breakdown field after 20 min plasma treatment is reduced by a factor of 2.5 relative to the initial value.

Figure 3 shows the results obtained from plasma-processed samples of equal thickness at different substrate temperatures for 20 min. As can be seen, by

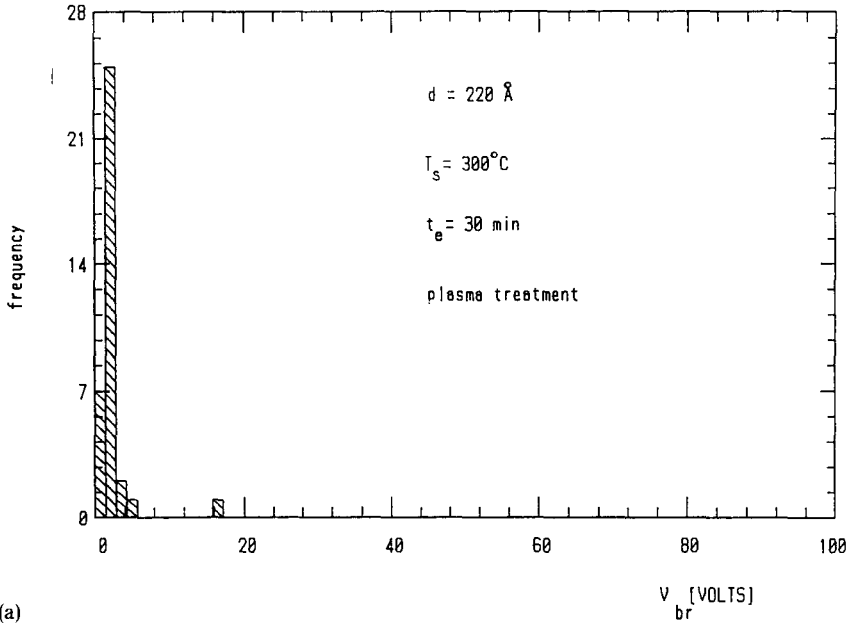


(a)

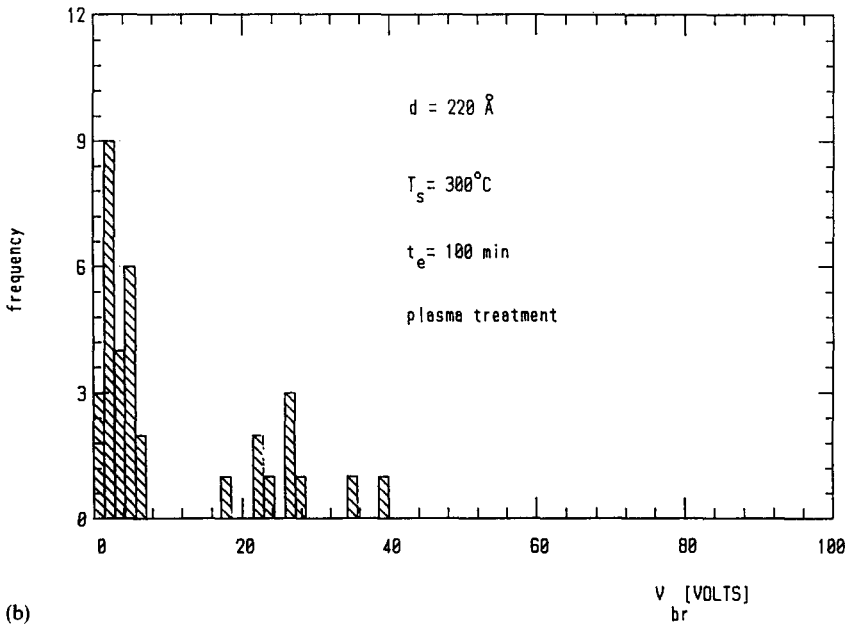


(b)

Fig. 3. Histograms of two samples,  $d = 220 \text{ \AA}$ , processed for 20 min in  $\text{NH}_3$  plasma at different substrate temperatures, (a)  $T_s = 100^\circ\text{C}$ , (b)  $T_s = 300^\circ\text{C}$ .



(a)



(b)

Fig. 4. Histograms of double-layer structure (a) with oxynitride layer thickness  $d_1 = 100 \text{ \AA}$  and SiO<sub>2</sub> thickness  $d_2 = 120 \text{ \AA}$  and (b) completely nitrified to oxynitride layer at  $T_s = 300^\circ\text{C}$  and  $t_e = 100 \text{ min}$  ( $d = 220 \text{ \AA}$ ).



increasing the temperature the breakdown voltage is considerably reduced, which indicates an increase in the concentration of plasma-created defects.

According to Auger and loss investigations of the layer stoichiometry<sup>6</sup>, after the action of  $\text{NH}_3$  plasma over  $\text{SiO}_2$  samples of thickness  $d = 220 \text{ \AA}$  at  $T_s = 300^\circ\text{C}$  the film is completely nitrated to oxynitride for  $t_e > 60$  min. For  $t_e = 30$  min (Fig. 4) the nitrated part of the thickness amounts to  $100 \text{ \AA}$  (measured from the outer surface of the layer). The stoichiometry of the layer corresponds to that of the typical oxynitride<sup>7</sup>  $\text{Si}_3\text{N}_3\text{O}_3$ . The underlying part of the layer is typical  $\text{SiO}_2$ . Therefore the plasma regime cited above can be used to obtain a double-layer structure  $\text{Si}_x\text{N}_y\text{O}_z/\text{SiO}_2$  with oxynitride layer thickness  $d_1 = 100 \text{ \AA}$  and  $\text{SiO}_2$  layer thickness  $d_2 = 120 \text{ \AA}$ . The mean breakdown field of this structure is about  $1.1 \times 10^6 \text{ V cm}^{-1}$ , which is nearly an order of magnitude lower than that of the as-grown  $\text{SiO}_2$  sample.

At a layer thickness of  $220 \text{ \AA}$  with  $t_e = 100$  min and  $T_s = 300^\circ\text{C}$ , a layer completely nitrated to oxynitride is obtained with a breakdown field  $E_{br} = 0.97 \times 10^6 \text{ V cm}^{-1}$ , which is an order of magnitude lower than the mean breakdown field of an as-grown sample with oxide thickness  $220 \text{ \AA}$ . Compared with the breakdown field of a double-layer structure of equal thickness ( $220 \text{ \AA}$ ), this value is about 40% lower.

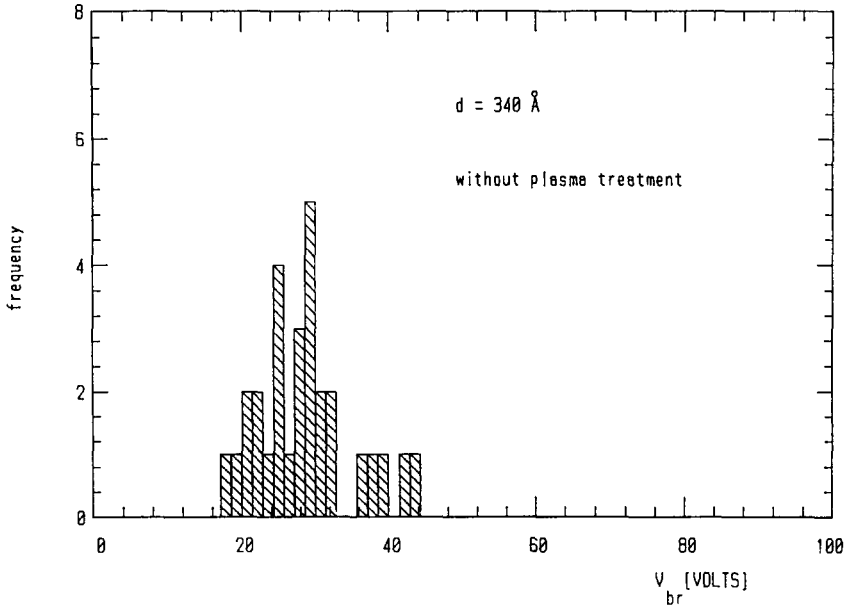
The films with thickness  $d = 340 \text{ \AA}$  cannot be nitrated to oxynitride for any duration of plasma nitridation (up to 100 min)<sup>7</sup>, even at the maximum substrate temperature used ( $T_s = 300^\circ\text{C}$ ). The plasma treatment results only in the creation of a thin nitrogen-enriched layer near the surface region of the oxide. The layer thickness is different depending on  $t_e$ . For  $t_e = 60$  min the thickness of the layer is  $30\text{--}40 \text{ \AA}$ . On increasing  $t_e$  to 100 min the thickness of the surface-enriched layer does not change any more, *i.e.* some kind of saturation of the nitridation process is observed. The histograms of an as-grown  $\text{SiO}_2$  film with oxide thickness  $d = 340 \text{ \AA}$  and of a double-layer structure fabricated with plasma treatment at  $T_s = 300^\circ\text{C}$  and  $t_e = 60$  min are shown in Fig. 5.

The corresponding mean breakdown field of the double-layer structure is  $E_{br} = 2.78 \times 10^6 \text{ V cm}^{-1}$  (Table I) and this sample has a very compact distribution ( $\sigma$  is relatively small), which means that the mean breakdown field is three times lower than that of the as-grown  $\text{SiO}_2$  sample. On the other hand, the breakdown voltage distribution of the double-layer structure is characterized by a smaller width compared to the original oxide breakdown voltage distribution.

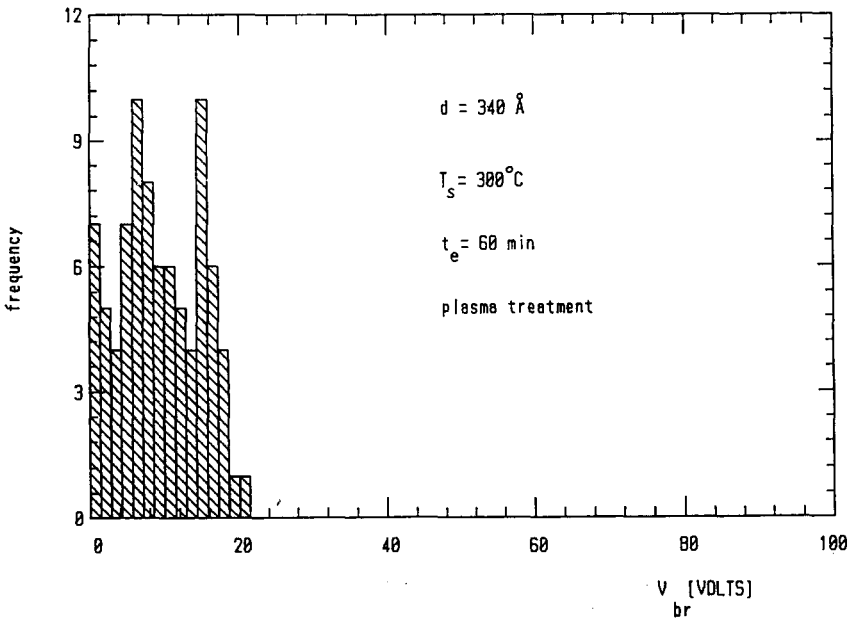
Fowler–Nordheim plots of the  $I$ – $V$  characteristics in the form of  $j/E^2$  vs.  $1/E$  are shown for illustration in Fig. 6 for one of the samples investigated ( $d = 340 \text{ \AA}$  before and after plasma treatment).

The plots of the nitrated samples at times of plasma exposure  $t_e > 2$  min are shifted to lower fields in comparison to the initial one. A linear regression analysis was performed (shown for illustration in Fig. 7 for one of the samples exposed to  $\text{NH}_3$  plasma) and the slopes given in Table II, column 2 have been obtained.

As can be seen from Fig. 6, the dependence for the initial  $\text{SiO}_2$  (signified by  $\circ$ ) is typical of Fowler–Nordheim emission (straight line). The character of the dependence  $j/E^2 = f(1/E)$  for plasma-irradiated samples (signified correspondingly by  $+$ ,  $\bullet$  and  $*$  in Fig. 6 and Table II) is very similar to the original one. The slopes of the curves (Table II, column 2) differ slightly. As has been pointed out, the technology

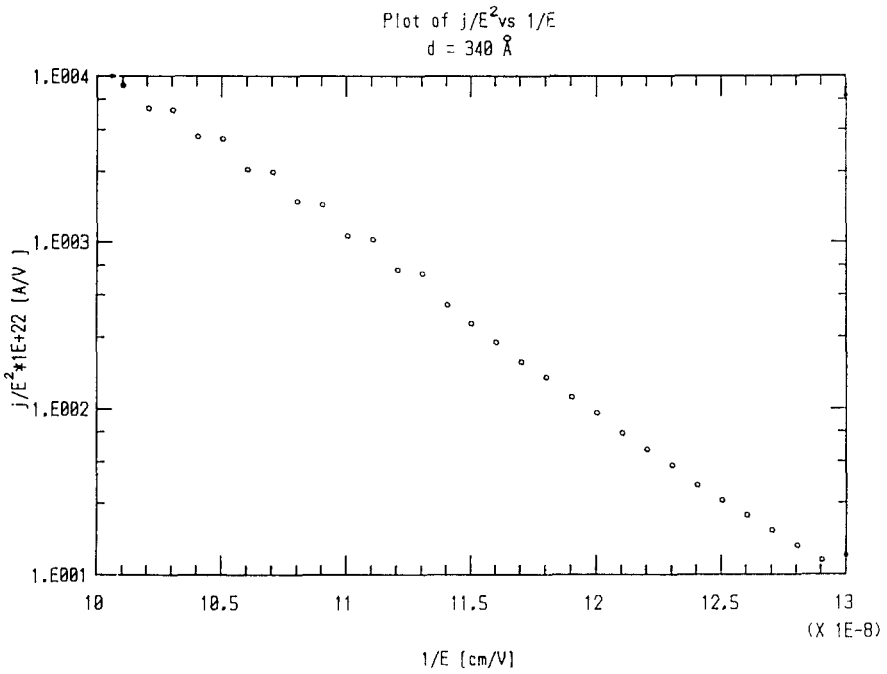
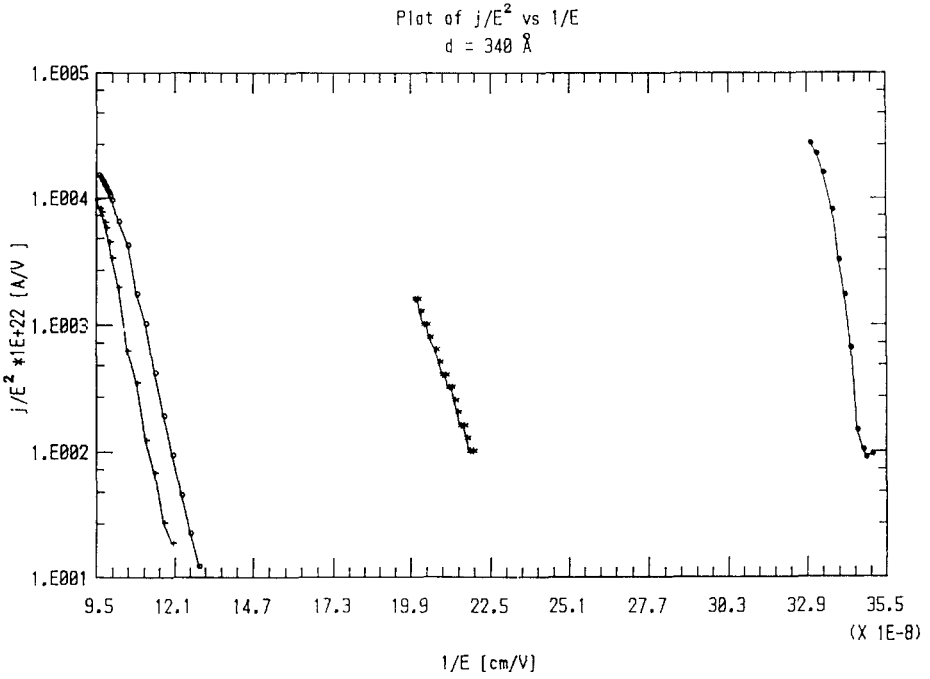


(a)



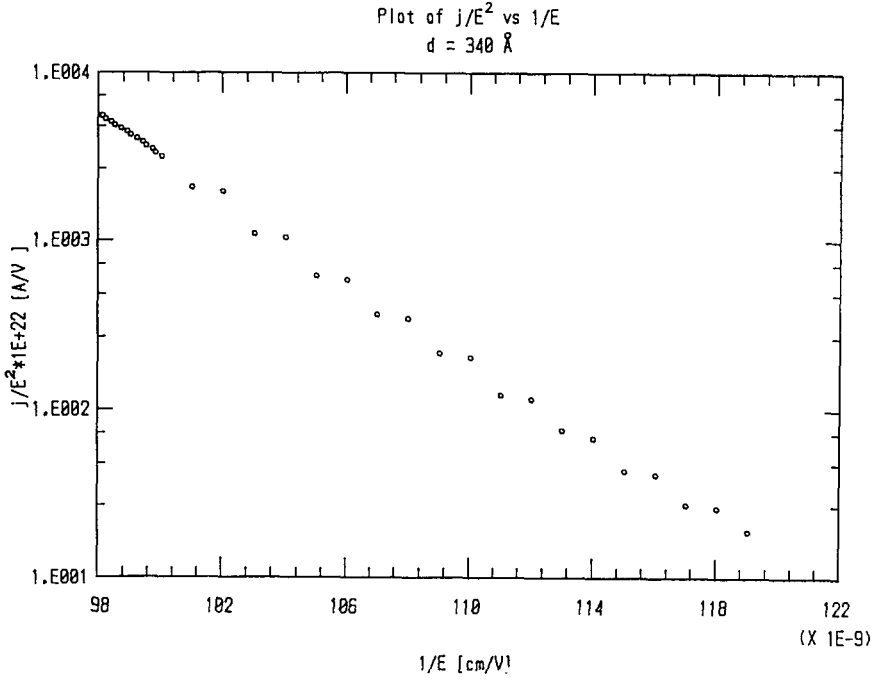
(b)

Fig. 5. Histograms of (a) as-grown SiO<sub>2</sub> sample with oxide layer thickness  $d = 340 \text{ \AA}$  and (b) equal-thickness double-layer structure with  $d_1 = 30\text{--}40 \text{ \AA}$  and  $d_2 = 300 \text{ \AA}$  ( $T_s = 300^\circ\text{C}$ ,  $t_e = 60 \text{ min}$ ).

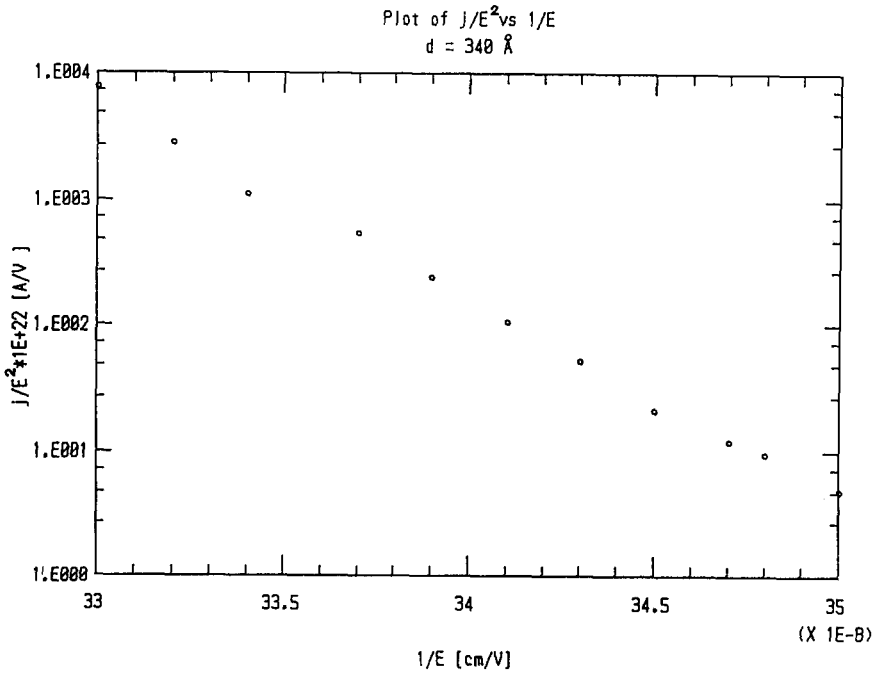


(a)

Fig. 6 (continued).



(b)



(c)

Fig. 6 (continued).

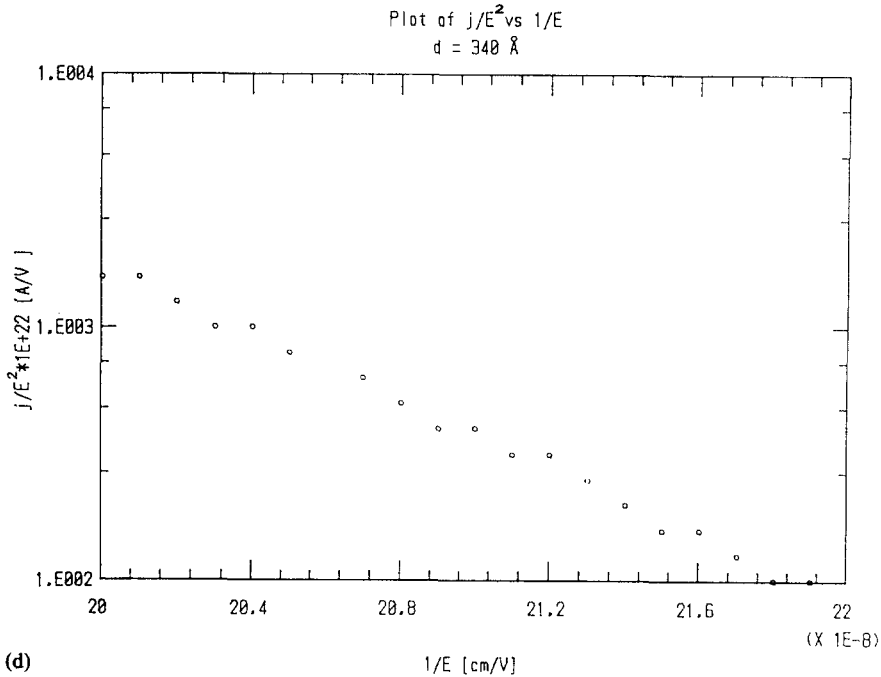


Fig. 6. Fowler–Nordheim plots of  $I$ – $V$  characteristics of as-grown  $\text{SiO}_2$  sample with oxide thickness  $d = 340 \text{ \AA}$  (a) before plasma treatment ( $\circ$ ) and (b)–(d) after plasma processing under different conditions: (b)  $+$ ,  $\text{NH}_3$  plasma,  $T_s = 200^\circ\text{C}$ ,  $t_c = 20$  min; (c)  $\bullet$ ,  $\text{NH}_3$  plasma,  $T_s = 200^\circ\text{C}$ ,  $t_c = 20$  min; (d)  $*$ ,  $\text{NH}_3$  plasma,  $T_s = 300^\circ\text{C}$ ,  $t_c = 60$  min.

conditions under consideration lead to a double-layer structure oxynitride/oxide ( $40 \text{ \AA} \text{ Si}_3\text{N}_3\text{O}_3/300 \text{ \AA} \text{ SiO}_2$ ). It is worth investigating the variation of the aluminium insulator barrier height with the technology conditions, assuming that the Fowler–Nordheim relation is valid. A similar approach for revealing the conduction mechanism is proposed by Cheng *et al.*<sup>6, 8</sup>. They have investigated thermally nitrated thin  $\text{SiO}_2$  (the initial oxide thicknesses of the samples investigated are close to those investigated in this paper— $195$  and  $335 \text{ \AA}$ ).

According to Cheng *et al.*<sup>8</sup>, for the electron effective mass in the oxynitride a value of  $m_{\text{Si}_x\text{N}_y\text{O}_z}/m = 0.5$  is acceptable ( $m$  is the free electron mass). Potential barrier heights  $\phi_b$  (Table II, column 3) have been calculated from the constant of Fowler–Nordheim emission

$$B = 6.83 \times 10^7 \left( \frac{m_{\text{ox}}}{m} \right)^{1/2} \phi_b^{3/2} \quad (\text{V cm}^{-1})$$

As can be seen (Table II), the barrier height is monotonously reduced compared to that of the system  $\text{Al-SiO}_2$  ( $\phi_b = 2.287 \text{ eV}$ ). After 60 min plasma treatment at  $300^\circ\text{C}$  the barrier height has been reduced by a factor of 2. This considerable decrease can be attributed to the resonant tunnelling mechanism through the bulk trap levels in the oxynitride layer generated by the  $\text{NH}_3$  plasma. This in turn can lead

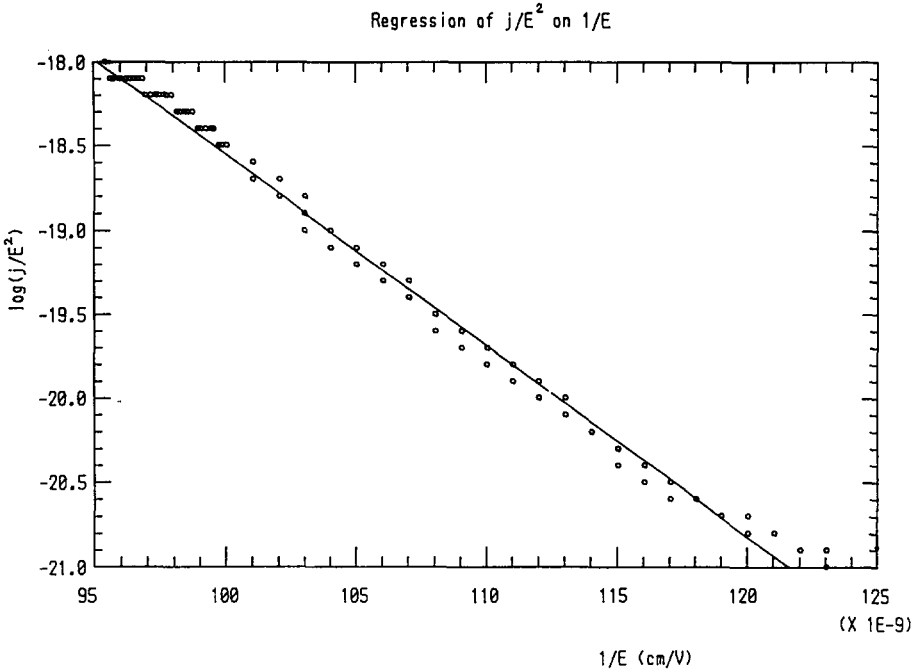


Fig. 7. Linear regression of  $\log(j/E^2)$  vs.  $1/E$  for sample processed in NH<sub>3</sub> plasma at  $T_s = 200^\circ\text{C}$  and  $t_e = 2$  min.

to a different type of conduction mechanism, *e.g.* Poole–Frenkel emission. In order to examine the possibility of parallel competing conduction mechanisms, the  $I$ – $V$  curves in Fig. 8 have been plotted for the same set of samples as in Fig. 6 in Poole–Frenkel coordinates, assuming the relation

$$j_{PF} = \text{const.} \times E \exp \left[ \frac{q}{kT} \left\{ \left( \frac{qE}{\pi\epsilon_0\epsilon_d} \right)^{1/2} - \Phi_T \right\} \right]$$

where  $\epsilon_0$  is the permittivity of free space,  $\epsilon_d$  is the dynamic dielectric constant and  $\Phi_T$  is the trap energy level from the insulator band edge.

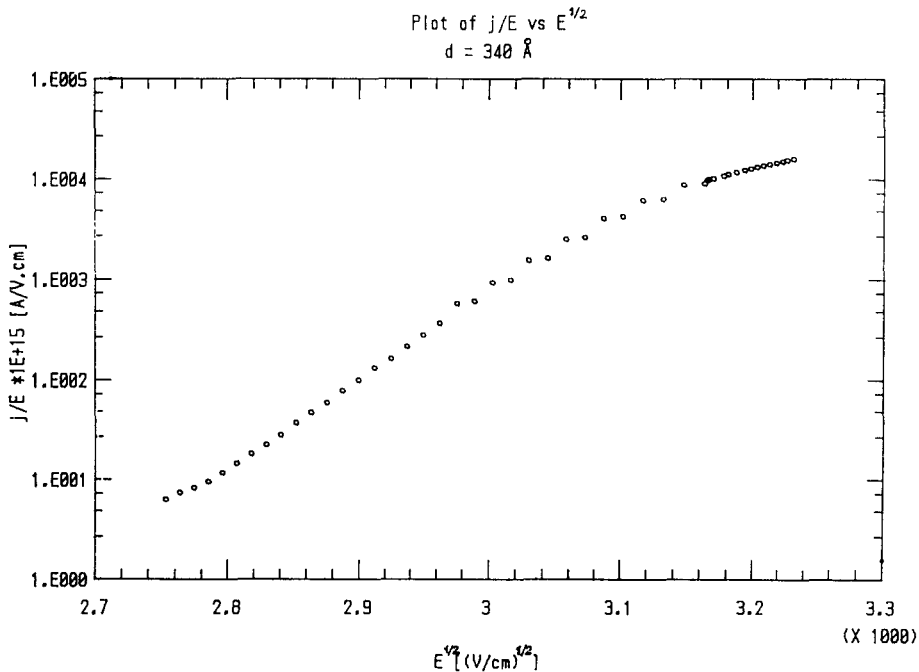
It can be clearly seen that the  $j/E$  vs.  $E^{1/2}$  dependence differs from the linear one. A conclusion which can be derived from Figs. 6 and 8 is that the existence of the traps does not alter the conduction mechanism for the investigated double-layer dielectric relative to the conduction mechanism of the as-grown oxide. One of the possible reasons for the reduction in barrier height in double-layer structures might be the modified Fowler–Nordheim tunnelling mechanism through the potential barrier with more complex shape. This complex shape is probably due to the build-up of positive charges during the process of nitridation in the bulk of the layer<sup>8</sup> and to the difference between the energy band gap of the oxynitride layer and that of the underlying thermal oxide. This is the reason why we use the term modified Fowler–Nordheim emission for the dominant conduction mechanism in the double-layer structures investigated. This does not exclude the parallel hopping conduction

with the assistance of bulk traps. The observed lower breakdown field of the double-layer structure relative to the breakdown field of the initial  $\text{SiO}_2$  can be attributed to the presence of bulk traps in the oxynitride. A more precise investigation of the conduction mechanism of such double-layer structures as a function of the ratio

TABLE II

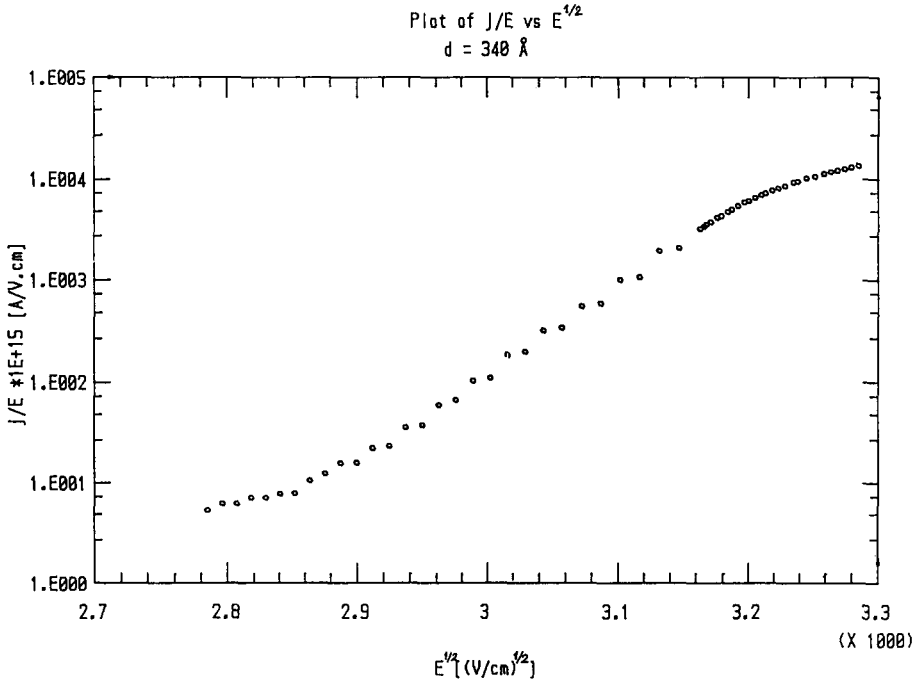
LINEAR REGRESSION ANALYSIS OF THE DEPENDENCE  $j/E^2$  vs.  $1/E$  FOR THE MEAN SLOPES AND CORRESPONDING BARRIER HEIGHTS OF THE SAMPLES, SHOWN IN FIG. 6 BY  $\circ$ ,  $+$ ,  $\bullet$ ,  $*$ . THE TECHNOLOGY CONDITIONS ARE ALSO GIVEN

Technology conditions	$B(\text{V cm}^{-1})$	$\phi_b(\text{eV})$
As-grown $\text{SiO}_2(d = 340 \text{ \AA})$	$-1.6686 \times 10^8$	2.287
$\text{NH}_3$ plasma $T_s = 200 \text{ }^\circ\text{C}$ $t_c = 2 \text{ min}$	$-1.6143 \times 10^8$	2.236
$\text{NH}_3$ plasma $T_s = 200 \text{ }^\circ\text{C}$ $t_c = 20 \text{ min}$	$-1.1850 \times 10^8$	1.819
$\text{NH}_3$ plasma $T_s = 300 \text{ }^\circ\text{C}$ $t_c = 60 \text{ min}$	$-6.5590 \times 10^7$	1.226

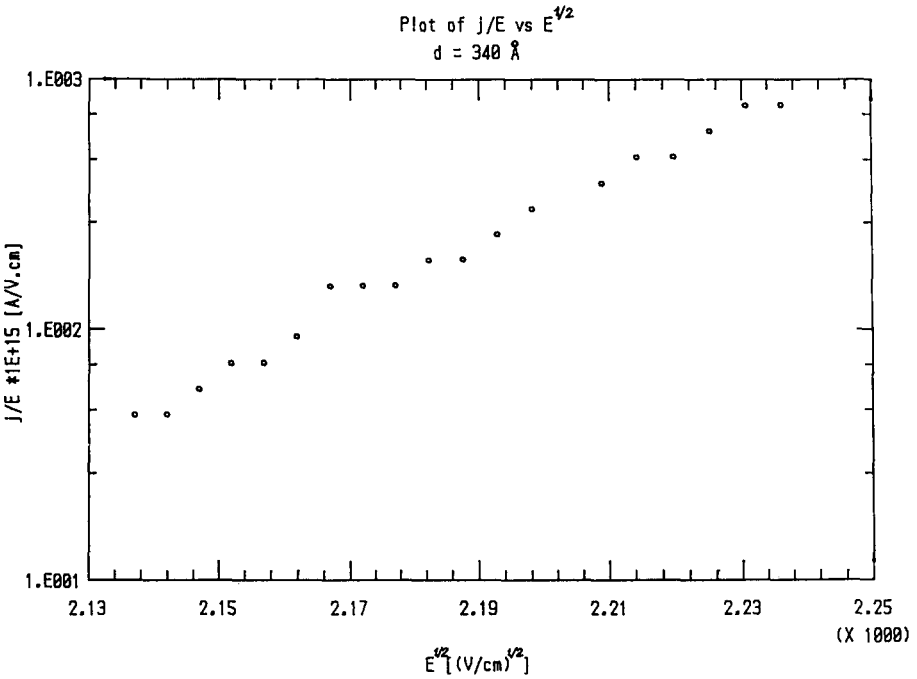


(a)

Fig. 8 (continued).



(b)



(c)

Fig. 8 (continued).



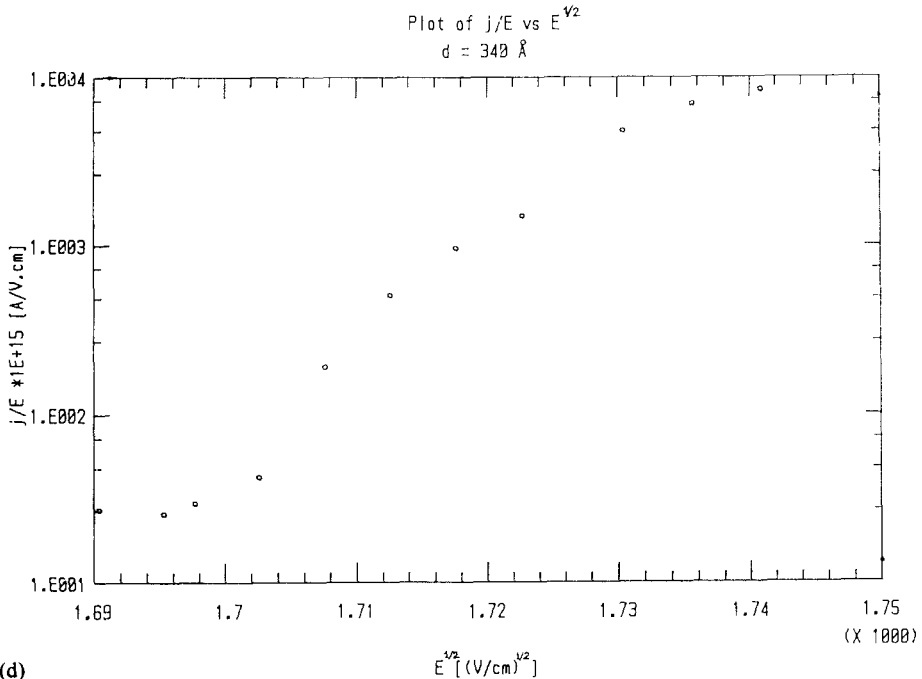


Fig. 8. Poole-Frenkel plots of the same  $I-V$  characteristics as in Fig. 6.

between the oxynitride and oxide thicknesses and its dependence on the plasma regime parameters will be the subject of further work.

#### 4. CONCLUSION

From the above results a conclusion can be deduced that generally the dielectric breakdown strength of plasma-nitrided chlorine oxides is reduced relative to the thermally grown oxide. Analysis of  $I-V$  curves in Fowler-Nordheim and Poole-Frenkel coordinates clearly shows that the former mechanism is responsible for the conductivity. The conduction mechanism for the examined samples changes from typical Fowler-Nordheim for the initial  $\text{SiO}_2$  sample to a modified Fowler-Nordheim tunnelling mechanism (*i.e.* with a reduced potential barrier height) for samples with a surface nitrogen-enriched oxide layer.

#### REFERENCES

- 1 F. H. P. M. Habraken, *Appl. Surf. Sci.*, **30** (1987) 186.
- 2 G. A. Ruggles and J. R. Monkowski, *J. Electrochem. Soc.: Solid State Sci. Technol.*, **133** (1986) 787.
- 3 S. S. Wong, C. G. Sodini, T. W. Ekstedt, H. R. Grinolds, K. H. Jackson, S. H. Kwan and W. G. Oldham, *J. Electrochem. Soc.*, **130** (1983) 1134.
- 4 T. Ito, T. Nakamura and H. Ishikawa, *J. Electrochem. Soc.*, **129** (1982) 184.
- 5 A. A. Yankova, Nitridation of thin  $\text{SiO}_2$  films, *Ph.D. Thesis*, Institute of Microelectronics, Sofia, 1988, p. 19.

- 6 X. R. Cheng, Y. C. Cheng and B. Y. Liu, *J. Appl. Phys.*, 63 (1988).
- 7 E. Atanassova and A. Shopov, private communication, 1989.
- 8 X. R. Cheng, B. Y. Liu and Y. C. Cheng, *Appl. Surf. Sci.*, 30 (1987) 237.